Academic Journal of Science and Technology
ISSN: 2771-3032 | Vol. 10, No. 1, 2024

Characterization of Surface Pressure Accuracy and Spatial and Temporal Variations of The GPT3 And HGPT2 Models in The Chinese Region

Sen Li*, Kai Wang, Haofei Ban, Chen Xue, Yongxiao Guo

College of Surveying, Mapping and Land Information Engineering, Henan Polytechnic University, 454003, China
*Correspondence: 212104020069@home.hpu.edu.cn

Abstract: The accuracy of surface pressure is crucial for obtaining high-precision zenith hydrostatic delay(ZHD). In order to verify the accuracy of the Global Pressure and Temperature model (HGPT2) and the Global Pressure and Temperature (GPT3) in obtaining ground air pressure in China, as well as the spatiotemporal variation characteristics of the errors of the two models, this paper uses the ERA5 reanalysis dataset and combines it with actual meteorological data from weather stations to evaluate their performance. The results show that the results show that the HGPT2 model has better accuracy in simulating atmospheric pressure in China than the GPT3 model, with atmospheric pressure bias of -0.54 hPa and -2.09 hPa, and RMS of 4.42 hPa and 4.91 hPa, respectively. This article analyzes the spatial and temporal characteristics of model errors based on China's climate types. The performance of the GPT3 and HGPT2 models varies in different regions, and their accuracy in simulating atmospheric pressure changes is poorer in northern and northwestern China.

Keywords: GPT3, HGPT2, Precision analysis, Surface pressure.

1. Introduction

Pressure plays a crucial role in calculating zenith hydrostatic delay within the Global Satellite Navigation System (GNSS) technology. This is pivotal for determining GNSS precipitable water vapor (PWV), as well as real-time monitoring and assessment of atmospheric water vapor content(Chen & Liu, 2016; Ding, 2020; Huang et al., 2021). It also holds significance in meteorological hazard monitoring, weather forecasting, and evaluating atmospheric quality (Lee, 2013; H. Li et al., 2021; Zhang et al., 2015; Zhu et al., 2023). Therefore, the study of obtaining high-precision pressure data is of utmost importance.

While meteorological parameters like surface pressure and air temperature can be accurately measured by weather stations, obtaining water vapor data with high spatial and temporal resolution remains challenging due to the high operational costs of conventional sensors such as radio sounders, weather radars, and water vapor radiometers (Bock et al., 2013; Guerova et al., 2016). As the number of GNSS stations equipped with meteorological sensors is limited, the global pressure-temperature model is primarily used to obtain data like air temperature and pressure across the globe. Initial atmospheric parameter correction models, such as the University of New Brunswick (UNB) series of models in Canada (Li et al., 2012; Wang & Li, 2016; Yao et al., 2015), suffered from poor spatial resolution due to a scarcity of early meteorological observing stations. This situation improved with the introduction of Numerical Weather Models (NWM). The GPT (global pressure and temperature) model family (Boehm et al., 2007; Zhang et al., 2018) which is based on reanalyzed NWP products from the European Centre for Medium-Range Weather Forecasting (ECMWF), is widely used. This series of models has been refined with increasing NWP spatial and temporal resolution, leading to improvements like GPT2, GPT2w, and GPT3 (Böhm et al., 2014; Lagler et al., 2013; Landskron & Böhm, 2017). GPT2w (Liu et al., 2017; Liu et al., 2019) refines GPT2 by incorporating a 1°×1° parameter file and introducing weighted mean temperature and water vapor decreasing factor parameters. GPT3, the latest iteration, includes an estimation of hydrostatic force gradients in various directions and has undergone rigorous evaluation and refinement by scholars (Ding & Chen, 2020; Huang et al., 2022; L. Li et al., 2022; S. Li et al., 2022), positioning it as the most accurate model in the series, widely employed in GNSS processing software like GAMIT/GLOBK and Bernese. HGPT employs the 20-year ECMWF ERA5 reanalysis with a 0.25° × 0.25° spatial and 1-hour temporal resolution. The HGPT(Cai et al., 2022; Mateus et al., 2020; Zhao et al., 2023) introduces a linear trend to provide surface pressure, temperature, zenithal non-hydrostatic delays, and weighted mean temperature values globally. In contrast, the HGPT2 (Mateus et al., 2021) is based on the time-split concept, offering information on relative humidity, zenith non-hydrostatic delay, and precipitable precipitation on a global scale with annual, semi-annual, and quarterly cycles. The model's performance significantly impacts the accuracy of solving ZHD and calculating PWV (L. Li et al., 2021; Wang et al., 2017; Xia et al., 2022). To assess the performance of the GPT3 and HPGT2 models in the Chinese region, this study utilizes the single-layer pressure products from the ERA5 reanalysis dataset. It combines the US Geological Survey (USGS) DEM grid data to obtain ground-level pressure for both models. The accuracy of the model-generated ground-level pressure is evaluated using actual measured pressure data from ground meteorological stations and vertically interpolated reanalysis dataset. This evaluation aims to determine the real-time atmospheric pressure model that demonstrates the most stable performance in the Chinese region. Additionally, the study analyzes the impact of different climatic types on model performance, providing reference for future model refinement research and enhancing model performance based on climatic characteristics. Since

the accuracy of atmospheric pressure estimation is crucial for the accuracy of calculating ZHD and PWV, the precision evaluation of the models is of great importance.

2. Data Sources and Methods

2.1. Data sources

The dataset employed encompasses 723 ERA5 grid points and 45 randomly chosen meteorological stations across China. Additionally, the USGS-provided DEM grid product was utilized to determine the elevation of the ground surface at the ERA5 grid points. The spatial arrangement of these elements is visualized in Figure 1.

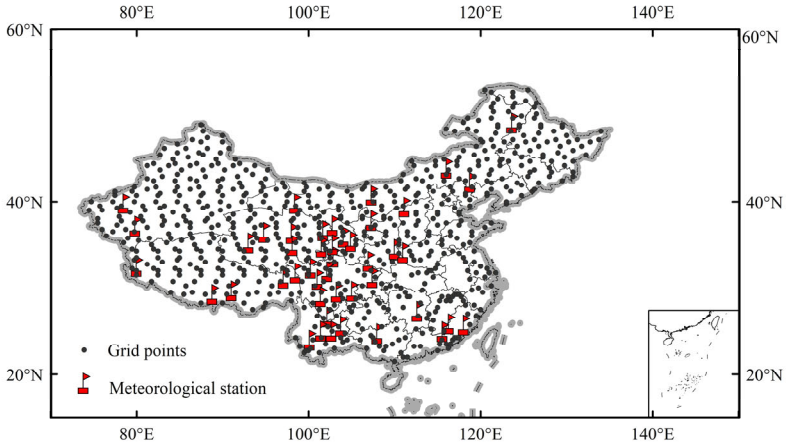

Figure 1. Illustrates the distribution of ERA5 grid points and weather station locations

2.2. Data Introduction

The dataset utilized for this research is sourced from the fifth-generation reanalysis dataset ERA5 (https://cds.climate.copernicus.eu/), which is published by the European Centre for Medium Range Weather Forecasts (ECMWF). This dataset spans from the year 1979 to the present. The ERA5 monolayer data consists of hourly records, often referred to as "land data". These records maintain a temporal resolution of 1 hour and are characterized by a horizontal resolution of 0.25° × 0.25°.Within the ERA5 ground data, essential variables like potential, surface pressure, and temperature are encompassed. These variables play a pivotal role in deriving pressure at ground-level points.Ground-based meteorological stations employ meteorological sensors to capture parameters such as air temperature, pressure, and total rainfall. The precision of pressure detection achieved by these stations is as high as 0.5 hPa. In this study, meteorological data sourced from the National Oceanic and Atmospheric Administration (NOAA) of the United States (https://www.noaa.gov/climate) are used for comparative analysis. Specifically, the accuracy of pressure measurements taken from 45 meteorological stations within the Chinese region is contrasted with pressure corrected using ERA5 single-layer pressure data. This study also incorporates a Digital Elevation Model (DEM) grid product sourced from the U.S. Geological Survey (USGS) (https://earthexplorer.usgs.gov/). With an approximate accuracy of 30 meters, this DEM grid product contributes to the research by providing elevation at the surface of the ERA5 grid points. These elevation are crucial for height corrections applied to the surface pressure within the ERA5 single-layer pressure product.

2.3. Two global pressure-temperature models

The GPT3 model (https://vmf.geo.tuwien.ac.at/codes/) represents the most recent advancement within the GPT model series. It furnishes global meteorological grid parameters, encompassing pressure (P), temperature (T), weighted mean temperature (T_m), and specific humidity (e). These parameters are provided at spatial resolutions of 1°×1° and 5°×5° for various grid points. The model employs the least squares method to estimate alterations in mean, annual, and semiannual values. The parameter derivation formula, represented by Equation (1), is provided as follows:

$$\mathrm{r}(t) = A_0 + A_1 \sin(\frac{DOY}{365.25}2\pi) + B_1 \sin(\frac{DOY}{365.25}2\pi) + A_2 \sin(\frac{DOY}{365.25}4\pi) + B_2 \sin(\frac{DOY}{365.25}4\pi) \quad (1)$$

where DOY stands for Days of Yearly Accumulation, andA_0, A_1, B_1, A_2, and B_2 are model parameters, all stored as ASCII codes.

The HGPT2 model(https://github.com/pjmateus/hgpt_model/releases) represents a significant advancement by being the first global model to make use of ERA5's full horizontal and temporal resolution. In comparison to previous reanalysis data products, ERA5 exhibits substantial enhancements in terms of horizontal grid spacing, number of vertical layers, and temporal resolution. This heightened temporal resolution has increased from 6 hours to 1 hour, thereby facilitating a more accurate representation of the water vapor dynamics process. The HGPT2 model adheres to the concept of temporal partitioning by incorporating the mean value along with three periodic functions that account for the cyclic patterns of yearly, semiannual, and quarterly periods. The parameter specified in Equation (2) is derived from the equation, and the formula is as follows:

$$r(t) = a_0 + a_1 \cdot \cos(\frac{2\pi \cdot (t - t_0)}{365.25} + f_1) + a_2 \cdot \cos(\frac{2\pi \cdot (t - t_0)}{182.63} + f_2) + a_3 \cdot \cos(\frac{2\pi \cdot (t - t_0)}{91.31} + f_3) \quad (2)$$

where a_0, a_1, a_2, and a_3 are the annual, semi-annual, and quarterly mean amplitudes, respectively, t is the Modified Julian Date (MJD), $t_0$is the MJD of the first observation, and f_1, f_2, and f_3 are the annual, semi-annual, and quarterly

initial values, respectively.

2.4. Methodology

Due to the different elevation systems used by the models, it is important to ensure uniformity in the calculation process. In this study, all elevations are converted to geopotential height. The formula for the standardized elevation calculation is as follows:

ERA5 reanalysis data uses geopotential which needs to be converted into geopotential height using Equation (3), which is provided below:

$$GPH = GP / g \tag{3}$$

where GPH is the geopotential height, GP is the geopotential, and g is the gravitational acceleration, taken as a constant 9.80665 $\mathrm{m/s^2}$

The GPT3 model uses Ellipsoidal height, which should be converted to orthometric height using Equation (4), which is as follows:

$$H_{正} = H - N \tag{4}$$

In this context, H refers to the GNSS ellipsoidal height, $H_{正}$ indicates the orthometric height, and N signifies the geoid undulation. The geoid undulation N is often computed using the EGM2008 (Earth Gravitational Model 2008) model released by the National Geospatial Intelligence Agency (NGA) of the United States. Furthermore, the NGA provides an executable program, "hsynth_WGS84.exe," which facilitates the calculation of the geoid undulation N. This program can determine the geoid undulation N at a specific location based on the latitude and longitude information of the site.

To convert geopotential height to altitude, we use equation (5), which is as follows:

$$H_g = \frac{g_{\varphi} \cdot R_{\varphi} \bullet H_S}{g_0 (R_{\varphi} + H_S)} \tag{5}$$

where H_S is the orthometric height, g_{φ} and g_0 are the normal gravitational acceleration at latitude φ and 45°, respectively, and R_{φ} is the effective radius of the earth at latitude φ. g_0 takes the value of the constant 9.80665, and g_{φ} and R_{φ} can be computed by Equation (6) and Equation (7):

$$g_{\varphi} = 9.780325 \bullet \left[\frac{1 + 0.00193185 \bullet \sin^2(\varphi)}{1 - 0.00669435 \bullet \sin^2(\varphi)} \right]^{0.5} \tag{6}$$

$$R_{\varphi} = \frac{6378.137}{1.006803 - 0.006706 \bullet \sin^2(\varphi)} \tag{7}$$

The geopotential height of ERA5 reanalysis data is not coincident with the ground, but has a vertical distance gap. In order to assess the accuracy of the HGPT2 and GPT3 models in calculating surface air pressure, this study corrects the meteorological data of the pressure layer to the ground by vertical interpolation. Formula (8) represents the vertical interpolation formula for air pressure, and formula (9) calculates the gravity value at that point. (Wang et al., 2017).

$$P = P_E \left[\frac{T_E - \gamma (H_S - H_E)}{T_E} \right]^{\frac{g \bullet M}{R \bullet \gamma}} \tag{8}$$

$$g = 9.8063 \left\{ 1 - 10^{-7} \bullet \frac{H_E + H_S}{2} \left[1 - 0.0026373 \bullet \cos(2\varphi) + 5.9 \times 10^{-6} \bullet \cos^2(2\varphi) \right] \right\} \tag{9}$$

where P_E and T_E are the pressure and temperature at the grid point, H_E and H_S are the height and site elevation at the grid point, respectively; M is the molar mass of dry air, with a value of 0.0289655kg · $\mathrm{mol^{-1}}$; R is the ideal atmospheric constant, with a value of 8.31432 kg · $\mathrm{mol^{-1}}$; and γ is the rate of temperature decrease, with a value of 6.5℃/Km.

When the meteorological station locations do not coincide with grid points, the nearest four grid points to the station are identified using inverse distance weighted interpolation. First, the pressure values are adjusted to the station height using equations (8) and (9). Then, the inverse distance weighted interpolation is applied to obtain the pressure value at the station location. The formula for inverse distance weighted interpolation is as follows:

Equation (10) outlines the weighted formula used in this process.

$$P_S = \sum_{i=1}^{4} \overline{w_i} P_{si} \tag{10}$$

where w_i is the weighting factor, which can be calculated from equation (11)

$$\overline{w_i} = \frac{w_i^{-1}}{w_1^{-1} + w_2^{-1} + w_3^{-1} + w_4^{-1}} \tag{11}$$

where w_i is the ellipsoidal distance from the i-th grid point to the measurement site.

2.5. Evaluation indicators

To evaluate the performance of two models, bias and root mean square error (RMS) are used as accuracy metrics. bias reflects the deviation between the estimated values of the model and the true values, while RMS measures the stability of the model. The formulas for calculating bias and RMS are as follows:

$$BIAS = \frac{\sum_{i=1}^{n} d_{vv_i}}{n} \tag{12}$$

$$RMS = \sqrt{\frac{\sum_{i=1}^{n} d_{vv_i}^{\ 2}}{n}} \tag{13}$$

where v is the actual value, V_i is the observed value, and d_{vv_i} is the deviation of the observed value from the actual

value n is the number of observations.

3. Results and Discussion

3.1. Accuracy analysis of two models

In order to comprehensively reflect the performance of the GPT3 model and the HGPT2 model in the Chinese region, we randomly selected 723 grid points within the Chinese area. The pressure at each grid point was calculated using the GPT3 model and the HGPT2 model respectively, and compared with the pressure provided by ERA5. We calculated their bias and RMS, and the results are shown in Figure 2.

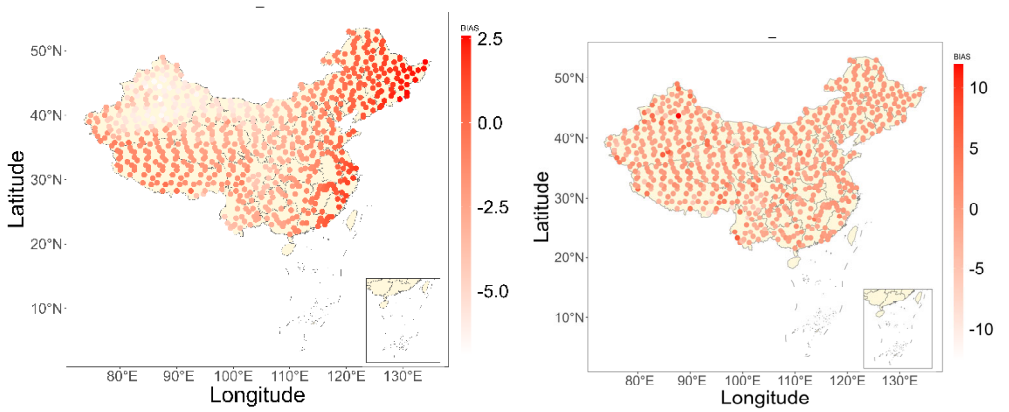

(a)bias

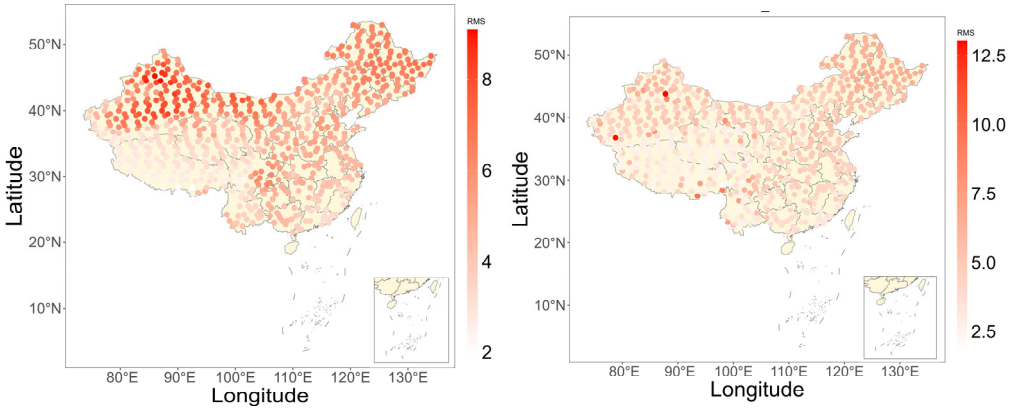

(b)RMS

Figure. 2. shows the bias and RMS for GPT3(left) and HGPT2 (right) in China

Table. 1. Comparison of accuracy of pressures calculated by GPT3 model and HGPT2 model

	GPT3/hpa	HGPT2/hpa
bias (MAX,MEAN,MIN)	[-6.87,-2.09,0.01]	[-12.97,-0.54,0.001]
RMS (MAX,MEAN,MIN)	[9.08,4.91, 1.94]	[13.04, 4.42, 1.81]

From Figure 2, it can be seen that in the China region, as compared to the ERA5 data, the HGPT2 model can better simulate the spatiotemporal variation patterns of atmospheric pressure, showing better performance. The calculated precision of atmospheric pressure is superior to that of the GPT3 model, the bias value being reduced by 74.1%, and the RMS value being reduced by 9.9%. This is not only due to the higher spatiotemporal resolution of the NWM product used by the HGPT2 model but also because the HGPT2 model is based on the ERA5 data for modeling, giving it an advantage. This explains the excellent bias performance of the HGPT2 model. To avoid interference caused by known differences between the two reanalysis datasets, the subsequent analysis in this study will interpolate the air pressure from the two models to meteorological stations, and the accuracy will be analyzed based on the observed air pressure data from the meteorological stations. Both models exhibit improved accuracy in the Qinghai-Tibet region and the low-latitude area. Nonetheless, regional discrepancies are evident. The accuracy of the GPT3 model weakens in the Northwest, while the HGPT2 model encounters challenges in the Northeast.

3.2. Accuracy analysis of two models in different climates

Different climate types are determined by factors such as terrain, latitude and longitude, as well as elevation, and they result in varying degrees of tropospheric variation. During the modeling of tropospheric models, it is challenging for physical formulas to accurately represent the fluctuation of the troposphere, leading to significant differences in model performance due to different climate types. To investigate the performance of the GPT3 and HGPT2 models in different regions of China, we have categorized the Chinese region into four areas based on climate types, namely: Northern region(N) is Temperate monsoon climate, Northwest region (N_w) is Temperate continental climate, Southern region (S) is Subtropical monsoon climate, and Qinghai-Tibet region (Q_T) is Plateau mountain climate, as shown in the figure 3.

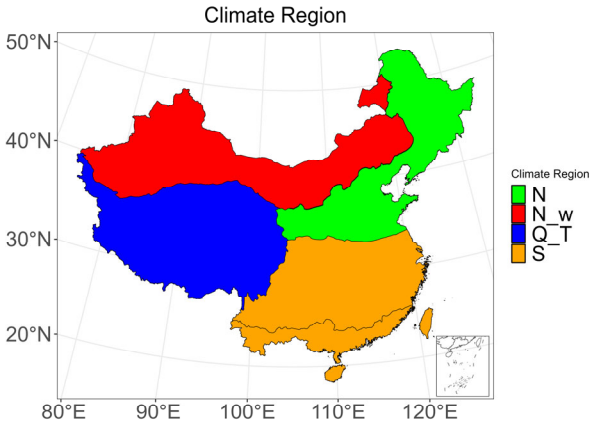

Figure 3. Climate Distribution Map of China

Different climates exhibit varying degrees of tropospheric activity, and this paper analyzes the performance of the two models in different climate regions of China. Figure 4 (a) shows the model accuracy in different climatic regions of China for two models. The results show when simulating pressure changes, the weather will significantly affect the simulation results. The two models perform relatively well in the southern and Qinghai-Tibet regions, with the best RMS performance in the Qinghai-Tibet region. However, as the latitude increases, the precision of the models begins to decrease, with the worst performance in the northwest region. The variation of atmospheric pressure in regions with high latitudes is more complex, making it harder to be represented by simple physical models. Figure 4(b) demonstrates the performance of two models in calculating surface air pressure in different climatic regions of China. It is evident from the figure that the performance of the GPT3 model is quite stable while the HGPT2 model has a significant performance difference in different climate regions, especially in the Qinghai-Tibet region, where the precision of the model experienced an unusual change, and the RMS exceeded 40hPa, resulting in significant deviation from actual pressure.

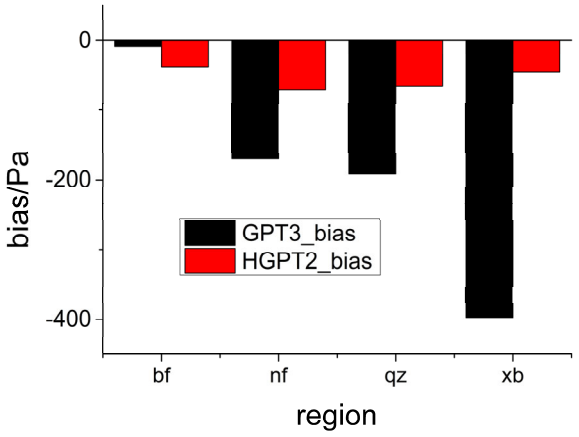

(a)

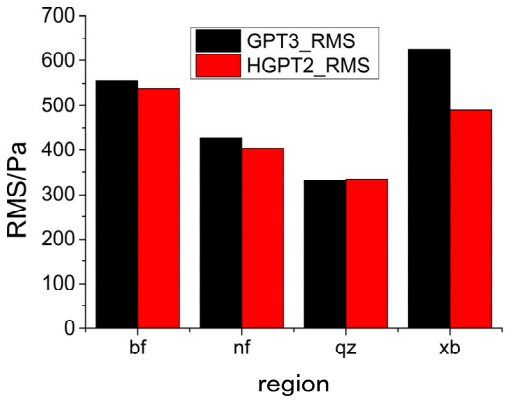

(b)

Figure 4. Accuracy of Two Models in Different Climate Regions, Figure (a)shows the accuracy of different models in different regions, Figure (b) shows the performance of ground air pressure in different regions.

3.3. Comparison with measured meteorological stations

In order to assess the effectiveness of both the GPT3 and HGPT2 models, validate the credibility of ERA5 data evaluation, and confirm the considerable variability in the accuracy of HGPT2 after surface correction, daily mean pressure data from 45 meteorological observation stations across China were employed for comparative analysis. Bias and RMS of the two models were computed individually. The geographical distribution of the meteorological station sites and their respective accuracy is illustrated in Figure 5:

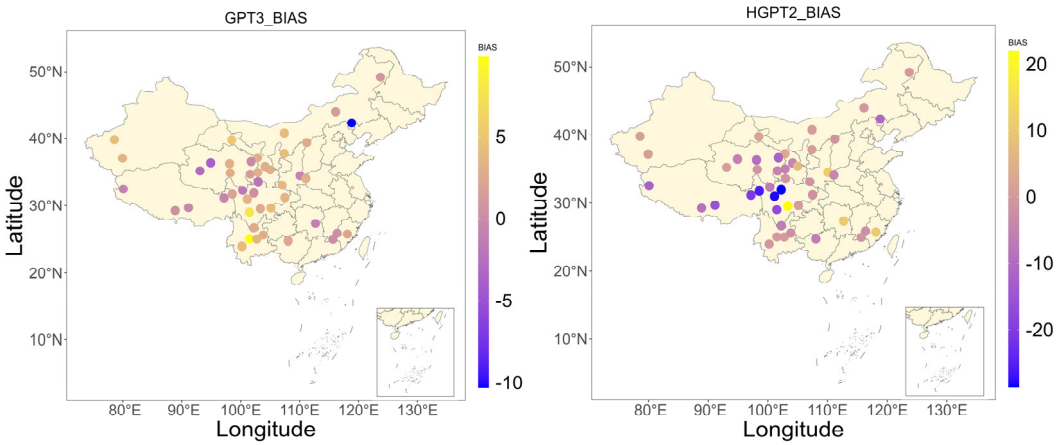

(a)bias

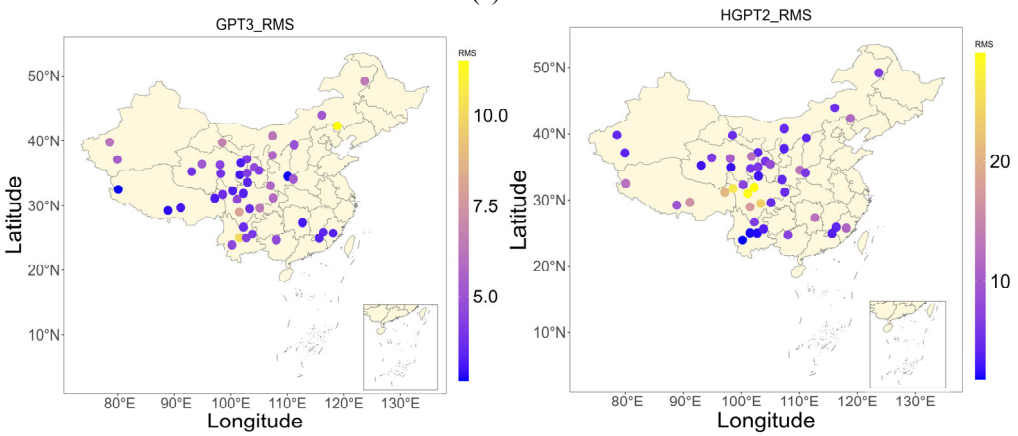

(b)RMS

Figure 5. Illustrates the comparison of accuracy between the weather station site pressure and the pressure calculated by the GPT3 model (left) and HGPT2 model (right) in China.

Table 2. Comparison of GPT3 and HGPT2 Calculated Weather Station Site Pressure and Weather Station Pressure Accuracy

	GPT3(hpa)	HGPT2(hpa)
bias	1.8	-3.84
RMS	4.71	8.81

Taking into account the known differences between the reanalysis data models, this study further validates the performance of the GPT3 model and HGPT2 model in obtaining surface pressure by using measured pressure data from meteorological stations. From Table 2, it can be seen that the overall accuracy of GPT3 is significantly better than HGPT2. Moreover, as shown in Figure 5, HGPT2 exhibits larger errors in calculating surface pressure in the Qinghai-Tibet region, consistent with the evaluation results using ERA5 mentioned earlier. Although HGPT2 has better accuracy in modeling, experimental results demonstrate that GPT3 outperforms HGPT2 in obtaining surface pressure.

4. Conclusion and Discussion

This study utilizes reanalysis data ERA5 and measured surface pressure data from meteorological stations to analyze the accuracy of the GPT3 model and HGPT2 model in China, as well as their performance in calculating surface pressure. The following conclusions are drawn based on the analysis of the spatial-temporal distribution characteristics of model errors.

This study utilized reanalysis data ERA5 and ground meteorological station measured data to analyze the accuracy of the GPT3 model and HGPT2 model in China, as well as the performance of the two models in simulating surface pressure. Through the analysis of the spatiotemporal distribution characteristics of model errors, the following conclusions were drawn: Both the HGPT2 model and GPT3 model demonstrated good performance in China, with the bias and RMS of the pressure in the HGPT2 model being superior to those of the GPT3 model. However, the HGPT2 model performed poorly at some station sites when simulating surface pressure. Furthermore, a comparison of the accuracy of the two models in different climate types indicated that

HGPT2 performed well in all climate types, while the GPT3 model had lower accuracy in the northwest region of China.

References

[1] Bock, O., Bosser, P., Bourcy, T., David, L., Goutail, F., Hoareau, C., Keckhut, P., Legain, D., Pazmino, A., Pelon, J., Pipis, K., Poujol, G., Sarkissian, A., Thom, C., Tournois, G., & Tzanos, D. (2013). Accuracy assessment of water vapour measurements from in situ and remote sensing techniques during the DEMEVAP 2011 campaign at OHP. Atmospheric Measurement Techniques, 6(10), 2777-2802. https://doi.org/10.5194/amt-6-2777-2013

[2] Boehm, J., Heinkelmann, R., & Schuh, H. (2007). Short Note: A global model of pressure and temperature for geodetic applications. Journal of Geodesy, 81(10), 679-683. https://doi.org/10.1007/s00190-007-0135-3

[3] Böhm, J., Möller, G., Schindelegger, M., Pain, G., & Weber, R. (2014). Development of an improved empirical model for slant delays in the troposphere (GPT2w). GPS Solutions, 19(3), 433-441. https://doi.org/10.1007/s10291-014-0403-7

[4] Cai, M., Li, J., Liu, L., Huang, L., Zhou, L., Huang, L., & He, H. (2022). Weighted Mean Temperature Hybrid Models in China Based on Artificial Neural Network Methods. Remote Sensing, 14(15). https://doi.org/10.3390/rs14153762

[5] Chen, B., & Liu, Z. (2016). A Comprehensive Evaluation and Analysis of the Performance of Multiple Tropospheric Models in China Region. IEEE Transactions on Geoscience and Remote Sensing, 54(2), 663-678. https://doi.org/10.1109/tgrs.2015.2456099

[6] Ding, J., & Chen, J. (2020). Assessment of Empirical Troposphere Model GPT3 Based on NGL's Global Troposphere Products. Sensors (Basel), 20(13). https://doi.org/10.3390/s20133631

[7] Ding, M. (2020). Reducing ZHD–ZWD mutual absorption errors for blind ZTD model users. Acta Geodaetica et Geophysica, 55(1), 51-62. https://doi.org/10.1007/s40328-019-00280-6

[8] Guerova, G., Jones, J., Douša, J., Dick, G., de Haan, S., Pottiaux, E., Bock, O., Pacione, R., Elgered, G., Vedel, H., & Bender, M. (2016). Review of the state of the art and future prospects of the ground-based GNSS meteorology in Europe. Atmospheric Measurement Techniques, 9(11), 5385-5406. https://doi.org/10.5194/amt-9-5385-2016

[9] Huang, L., Peng, H., Liu, L., Xiong, S., Xie, S., Chen, J., Li, J., & He, H. (2021). GNSS Precipitable Water Vapor Retrieval With the Aid of NWM Data for China. Earth and Space Science, 8(9). https://doi.org/10.1029/2020ea001550

[10] Huang, L., Zhu, G., Peng, H., Liu, L., Ren, C., & Jiang, W. (2022). An improved global grid model for calibrating zenith tropospheric delay for GNSS applications. GPS Solutions, 27(1). https://doi.org/10.1007/s10291-022-01354-9

[11] Lagler, K., Schindelegger, M., Böhm, J., Krásná, H., & Nilsson, T. (2013). GPT2: Empirical slant delay model for radio space geodetic techniques. Geophysical Research Letters, 40(6), 1069-1073. https://doi.org/10.1002/grl.50288

[12] Landskron, D., & Böhm, J. (2017). VMF3/GPT3: refined discrete and empirical troposphere mapping functions. Journal of Geodesy, 92(4), 349-360. https://doi.org/10.1007/s00190-017-1066-2

[13] Lee, S.-W. L. J. K. B. S. D. H. K. Y. J. (2013). Monitoring precipitable water vapor in real-time using global navigation satellite systems.pdf. ORIGINAL ARTICLE. https://doi.org/10.1007/s00190-013-0655-y

[14] Li, H., Wang, X., Wu, S., Zhang, K., Chen, X., Zhang, J., Qiu, C., Zhang, S., & Li, L. (2021). An Improved Model for Detecting Heavy Precipitation Using GNSS-Derived Zenith Total Delay Measurements. IEEE Journal of Selected Topics in Applied Earth Observations and Remote Sensing, 14, 5392-5405. https://doi.org/10.1109/jstars.2021.3079699

[15] Li, L., Gao, Y., Xu, S., Lu, H., He, Q., & Yu, H. (2022). The New Improved ZHD and Weighted Mean Temperature Models Based on GNSS and Radiosonde Data Using GPT3 and Fourier Function. Atmosphere, 13(10). https://doi.org/10.3390/atmos13101648

[16] Li, L., Wu, S., Zhang, K., Wang, X., Li, W., Shen, Z., Zhu, D., He, Q., & Wan, M. (2021). A new zenith hydrostatic delay model for real-time retrievals of GNSS-PWV. Atmospheric Measurement Techniques, 14(10), 6379-6394. https://doi.org/10.5194/amt-14-6379-2021

[17] Li, S., Xu, T., Xu, Y., Jiang, N., & Bastos, L. (2022). Forecasting GNSS Zenith Troposphere Delay by Improving GPT3 Model with Machine Learning in Antarctica. Atmosphere, 13(1). https://doi.org/10.3390/atmos13010078

[18] Li, W., Yuan, Y., Ou, J., Li, H., & Li, Z. (2012). A new global zenith tropospheric delay model IGGtrop for GNSS applications. Chinese Science Bulletin, 57(17), 2132-2139. https://doi.org/10.1007/s11434-012-5010-9

[19] Liu, J., Chen, X., Sun, J., & Liu, Q. (2017). An analysis of GPT2/GPT2w+Saastamoinen models for estimating zenith tropospheric delay over Asian area. Advances in Space Research, 59(3), 824-832. https://doi.org/10.1016/j.asr.2016.09.019

[20] Liu, Z., Chen, X., & Liu, Q. (2019). Estimating Zenith Tropospheric Delay Based on GPT2w Model. IEEE Access, 7, 139258-139263. https://doi.org/10.1109/access.2019.2931984

[21] Mateus, P., Catalão, J., Mendes, V. B., & Nico, G. (2020). An ERA5-Based Hourly Global Pressure and Temperature (HGPT) Model. Remote Sensing, 12(7). https://doi.org/10.3390/rs12071098

[22] Mateus, P., Mendes, V. B., & Plecha, S. M. (2021). HGPT2: An ERA5-Based Global Model to Estimate Relative Humidity. Remote Sensing, 13(11). https://doi.org/10.3390/rs13112179

[23] Wang, M., & Li, B. (2016). Evaluation of Empirical Tropospheric Models Using Satellite-Tracking Tropospheric Wet Delays with Water Vapor Radiometer at Tongji, China. Sensors (Basel), 16(2), 186. https://doi.org/10.3390/s16020186

[24] Wang, X., Zhang, K., Wu, S., He, C., Cheng, Y., & Li, X. (2017). Determination of zenith hydrostatic delay and its impact on GNSS-derived integrated water vapor. Atmospheric Measurement Techniques, 10(8), 2807-2820. https://doi.org/10.5194/amt-10-2807-2017

[25] Xia, P., Tong, M., Ye, S., Qian, J., & Fangxin, H. (2022). Establishing a high-precision real-time ZTD model of China with GPS and ERA5 historical data and its application in PPP. GPS Solutions, 27(1). https://doi.org/10.1007/s10291-022-01338-9

[26] Yao, Y., Zhang, B., Xu, C., He, C., Yu, C., & Yan, F. (2015). A global empirical model for estimating zenith tropospheric delay. Science China Earth Sciences, 59(1), 118-128. https://doi.org/10.1007/s11430-015-5173-8

[27] Zhang, K., Manning, T., Wu, S., Rohm, W., Silcock, D., & Choy, S. (2015). Capturing the Signature of Severe Weather Events in Australia Using GPS Measurements. IEEE Journal of Selected Topics in Applied Earth Observations and Remote Sensing, 8(4), 1839-1847. https://doi.org/10.1109/jstars.2015.2406313

[28] Zhang, W., Lou, Y., Huang, J., & Liu, W. (2018). A refined regional empirical pressure and temperature model over China. Advances in Space Research, 62(5), 1065-1074. https://doi.org/10.1016/j.asr.2018.06.021

[29] Zhao, L., Cui, M., & Song, J. (2023). An Improved Strategy for Real-Time Troposphere Estimation and Its Application in the Severe Weather Event Monitoring. Atmosphere. https://doi.org/10.3390/atmos14010046

[30] Zhu, D., Zhang, K., Sun, P., Wu, S., & Wan, M. (2023). Homogenization of daily precipitable water vapor time series.pdf. Advances in Space Research https://doi.org/10.1016/j.asr.2023.04.052